Volume 13, No.3 September 2000

ISSN 1000-9345
CODEN CJMEER

CHINESE JOURNAL ® of MECHANICAL ENGINEERING

(English Edition)

机械工程学报

The official journal of
Chinese Mechanical Engineering Society



Co-published by



China Machine Press

and



Springer

需要全本请访问 www.ertongbook.com

Editorial Advisory Board of English Edition

Honorary Chairmen: Lei Tianjue Wang Buxuan Pan Jiluan

Chairman: Zhang Qixian

Vice Chairmen: Xu Binshi Liu Fei Pan Xinhan Wu Guanchang

Members:

Becher Gerhard W
Der Bundesanstalt für Materialforschung und Prüfung, Unterden Eichen 87, 122203, Berlin, Bundesrepublik Deutschland

Beitz W
Technische Universitat Berlin
Straβe des 17, Juni 135 D-10623 Berlin

Bell Tim
School of Metallurgy and Materials, University of Birmingham, United Kingdom

Bian Xiufang Shandong University of Technology

Chen Xinzeng Ningbo College

Chen Xinzhao Hefei University of Technology

Chen Xuejun Xi'an Jiaotong University

Ding Chun
Research Institute of Machinery Science and Technology

Ding Peifan Chinese Mechanical Engineering Society

Doege Echart
Institut für Umformtechnik u. Umformmaschinen, Universität Hannover, Welfengarten 1 A 30167, Bundesrepublik Deutschland

Eversheim W Lehrstuhl für Produktionssystematik, Steinbachstr. 53B, D-52056 Aachen

Fu Lansheng
China Machinery Industry Information Institute

(Continued on the 3rd cover)

CHINESE JOURNAL OF MECHANICAL ENGINEERING

(English Edition) (Quarterly) (Started in 1988)
Volume 13 No.3 September 2000

Responsible Dept: China Association for Science and Technology
Sponsored by: Chinese Mechanical Engineering Society
Editor in Chief: Shi Zhiping
Executive Editor: Liang Fujun
Editorial Office: 22 Baiwanzhuang Dajie, Beijing 100037, China
Tel: 0086 - 10 - 68994557 0086 - 10 - 68326677 - 2421
Fax: 0086 - 10 - 68994557
http://www.machineinfo.gov.cn/cjme
E-mail: cjme@mail.machineinfo.gov.cn
Co-published by: China Machine Press and Springer-Verlag
Printed by: Beijing Beilin Printing House

Copyright: ©2000 China Machine Press and Springer-Verlag

The exclusive distributor in the territory of American continent:
The American Society of Mechanical Engineers
345 East 47th Street, New York, NY10017
Sole distributor outside China and the American continent:
Springer-Verlag

ISSN 1000—9345
CN 11—2737/TH

(Continued from the back cover)
Gan Dongying
Institute of Optics and Fine Mechanics, Chinese Academy of Sciences
Gao Zhongyu Qinghua University
Guo Dongming
Dalian Institute of Technology
Hu Zizheng Shanghai Railway University
Huang Shisheng
South China University of Science and Technology
Iida Kunihiro
Japan Power Engineering and Inspection Corporation, Shin-Toranomon BLDG
Jost H Peter
Angel Lodge Laboratories & Works, Eley Estate, London, N18 3DB, United Kingdom
Kopineck Hermann-Josef
Wildbannweg 36D-44229 Dortmund, Bundesrepublik Deutschland
Li Qingchun Harbin Institute of Technology
Li Rongbin
The Hong Kong Polytechnic University
Lian Yuanjian
State Administration of Mechinery Industry
Lin Shangyang
Harbin Research Institute of Welding
Liu Baicheng Qinghua Univeristy
Liu Cai Yanshan University
Liu Fei Chongqing University
Liu Yaohui Jilin Institute of Technology
Liu Zengdian
East China University of Technology
Liu Zhubai Yanshan University
Lu Yongxiang Chinese Academy of Sciences
Lu Zesheng Harbin Institute of Technology
Luo Jiashun Nankai University
Mao Qiande Beijing Institute of Technology
Mei Zhongqin
China Machinery Industry Information Institute
Ohashi Hideo
Kogakuin University, Tokyo 163-91, Japan
Pan Xinhan
Chinese Mechanical Engineering Society
Seireg Ali
University of Wisconsin, Madison, U.S.A.
Song Kongjie
Shandong University of Technology
Song Yuquan Jilin University of Technology
Tang Xiangyun Qinghua University
Wang Min
Nanjing University of Aeronautics and Astronautics
Wang Xiankui Qinghua University
Wen Bangchun Northeastern University
Wen Shizhu
National Tribology Laboratory, Qinghua University
Wu Guanchang
China Machinery Industry Information Institute
Xie Youbo Xi'an Jiaotong University
Xiong Youlun
Huazhong University of Science and Technology
Xu Binshi
Armoured Forces Engineering Institute
Yan Yongnian Qinghua University
Yang Jialing
Beijing University of Aeronautics and Astronautics
Yang Shuzi
Huazhong University of Science and Technology
Yu Xinlu Qinghua University
Zhang Bolin Guangdong University of Technology
Zhang Ce Tianjin University
Zhang Guanghui
State Key Laboratory of Mechanical Transmission, Chongqing University
Zhang Qixian
Beijing University of Aeronautics and Astronautics
Zhang Zhiming Shanghai University
Zhong Binglin The Education Ministry
Zhong Qunpeng
Beijing University of Aeronautics and Astronautics
Zhou Yaohe Shanghai Jiaotong University
Zhou Kongkang
Jiangsu University of Science and Technology

CHINESE JOURNAL OF MECHANICAL ENGINEERING

Volume 13 Number 3 2000

Contents

Lucia Umberto Physical model for the engineering analysis of the thermoelasticity of solid bodies 165

Zhan Yong et al Optimal feed rate control for multi-axis CNC machining of free form surfaces 171

Fu Xin et al Study on the periodic waterhammer initiated by a novel hydraulic shock generator 178

Zhang Bolin et al Zero transmission and its application in high speed CNC machine tools 184

Zhou Shouqin et al Analysis of coupling influences of labyrinth seal parameters on cross coupled stiffness and direct damping coefficient 190

Hang Hongzhong Calculation of fuzzy reliability in the case of random stress and fuzzy fatigue strength 197

Lei Hong et al Experimental study on tribological properties of fullerene copolymer nanoball 201

Wang Rongliang et al Study on an object-oriented feature-based CAD of hydraulic manifold block 206

Dai Jiansheng et al Metamorphic mechanisms and their configuration models 212

Song Wenwu et al Research and design of the Straflo-Franics turbine 219

Ye Yunyue et al New punching machine driven by linear induction motor 224

Jiang Lan et al Integrated control for vehicle yaw motion using double-cost-function LQR 228

Tan Dalong et al Study on sensor-based control method for harmonic drive system 234

Chen Yong et al Analysis of the deflection of reeds in automotive hydraulic shock absorbers 241

PHYSICAL MODEL FOR THE ENGINEERING ANALYSIS OF THE THERMOELASTICLTY OF SOLID BODIES

Lucia Umberto
I.N.F.M.-Istituto Nazionale per la Fisica della Materia, Nucleo Applicativo, Applied Physics and Technological Transter Office, at Parco Scientifico Tecnologico in Valle Scrivia, Strada Savonese Ioc. Rivalta Scrivia, I-15047 Tortona(AL), Italy

Abstract The thermal behaviour of the solids under elastic deformations is analysed in order to obtain a model which combines the molecular dynamics results with the global thermal behaviour of the solids under elastic transformations. The result obtained consists of the introduction of the thermal behaviour in the Parrinello-Rahman model, obtaining the thermal molecular dynamic model useful in the analysis of the thermoelastic behaviour of solids.

Key words: Thermoelasticity Stress Strain Molecular dynamics Thermophysical properties of materials

NOTATIONS

Latin letters

$\boldsymbol{a}$——Vector direction in the molecular dynamic cell
$\boldsymbol{b}$——Vector direction in the molecular dynamic cell
$\boldsymbol{c}$——Vector direction in the molecular dynamic cell
c——Specific heat capacity($J\cdot kg^{-1}\cdot K^{-1}$)
$\boldsymbol{D}$——Finite strain tensor
$\boldsymbol{E}$——Strain tensor
$\boldsymbol{G}$——Metric tensor
$\boldsymbol{h}$——Geometrical reference tensor in the molecular dynamic cell
L——Lagrangian(J)
m——Mass(kg)
N——Total number of particles
p——Hydrostatic pressure(Pa)
$\boldsymbol{q}$——Areic heat flow rate ($W\cdot m^{-2}$)
r——Position(m)
$\boldsymbol{s}$——Vector position in the molecular dynamic reference(m)
$\boldsymbol{S}$——Stress tensor($N\cdot m^{-2}$)
t——Time(s)
T——Temperature(K)
u——Vector displacement(m)
V——Global potential(J)
W——Arbitrary constant($kg\cdot m^2$)
x——Position component(m)

Greek letters

α——Linear thermal expansion coefficient(K^{-1})
$\beta=(3\lambda+2\mu)\alpha(N\cdot m^{-2}\cdot K^{-1})$
ε——Strain tensor components
ϕ——Local interaction potential(J)
η——s position component(m)
λ——Lame moduli($N\cdot m^{-2}$)
μ——Lame moduli($N\cdot m^{-2}$)
Ω——Volume of the molecula dynamic cell(m^3)

$$\boldsymbol{\pi}=\Omega^{-1}\sum_{k=1}^{N}m_k[(\boldsymbol{h}\dot{\boldsymbol{s}}_k)^+(\boldsymbol{h}\dot{\boldsymbol{s}}_k)]+\Omega^{-1}\sum_{k=1}^{N}\sum_{i>k}^{N}\left(\frac{\mathrm{d}\phi(r_{ki})}{\mathrm{d}r_{ki}}\boldsymbol{h}\frac{\boldsymbol{s}_k-\boldsymbol{s}_i}{r_{ki}}\right)(J\cdot m^{-3})$$

ρ——Mass density($kg\cdot m^{-3}$)
$\boldsymbol{\sigma}=\Omega\boldsymbol{h}_0^{+-1}(m^3)$
$\sum=\Omega\boldsymbol{h}_0^{+-1}(\boldsymbol{S}-p\boldsymbol{I})\boldsymbol{h}_0^{-1}(J)$
ξ——s position component(m)
X——Inner thermal source($J\cdot kg^{-1}\cdot K^{-1}$)
ζ——s position component(m)

Manuscript received on December 10, 1999

需要全本请访问 www.ertongbook.com

Superscripts

+ ——Transposed of a matrix

· ——First order time derivative

·· ——Second order time derivative

Subscripts

α ——α-th

β ——β-th

k ——k-th

i ——i-th

0——Reference

Symbols

I ——Identity or unit matrix

tr——Trace of a matrix

δ_{ki} ——Kronecker symbol $\begin{cases} 1 & \text{if } i = k \\ 0 & \text{if } i \neq k \end{cases}$

grad——Gradient(m^{-1})

div——Divergence(m^{-1})

0 INTRODUCTION

The thermodinamics of oxide solid solution plays an important role in many areas of pure and applied energy engineering and applied physics, including heterogeneus catalysis, sensors, high temperature superconductors and solid state batteries. Moreover where materials are sustained at high temperatures, wherein phase stability might be an important factor in determining materials performance, a knowledge of the thermodinamics is fundamental for successful technical engineering[1,2].

The use of high-tech materials for structural applications has shown in recent years that the study of mechanical behaviour of such materials is often inadequate. Studies on the interaction between mechanical and thermal effects in solid bodies have therefore received considerable attention[3].

The behaviour of solids under the combined effects of external stress and of temperature has considerable pratical rilevance. Yet even in the idealized case of perfect crystal, a detailed microscopic picture of such effects is still lacking. Most of the theoretical studies have been confined to conditions at zero temperature; Moreover a perfect and prefized crystalline arrangement of the atoms has been assumed. These two assumptions may lead to useful insights for relatively small values of the stress and temperature. However, it is interesting to study the behaviour of solids at normal temperatures and at high values of the external stress. In particular at high values of the stress spontaneous defect generation or crystal transformation become possible[5].

Recently the maximum principle of the irreversible entropy for the open systems has been demonstrated as a general principle of stability for the stationary states[5~7]. This principle has been appiled to the analysis of the solid materials obtaining results in agree with the other classical method of onvestigation, but it does not present any chemical or physical restrictions[2].

Here the thermal consequences of the elastic deformations will be considered obtanining a model that combines the molecular dynamics results with the global thermal behaviour of the sloid in order to obtain a theoretical and numerical method usefull in appilcation in mechanical and energy engineering, in material science and engineering, in chemical engineering and in applied physics. To do that in section 1 an introduction to Molecular dynamics will be presented, in section 2 the results of Parrinello and Rahman will be summerised, in section 3 the thermodynamic analysis of the linear thermoelastic bodies will be developed and in section 4 the thermoelastic molecular dynamic model will be presented.

1 FUNDAMENTALS OF MOLECULAR DYNAMICS

Molecular dynamics is a method for studying classical statistical mechanics of well defined systems

through a numerical solution of Newton's equations.

Let us consider a set of N classical particles with coordinates $\boldsymbol{r}_i$, velocities $\dot{\boldsymbol{r}}_i$ and masses m_i with $i = 1, \cdots, N$. These particles interact through a potential[8]

$$V = \frac{1}{2}\sum_{i=1}^{N}\sum_{j=1}^{N}\phi(r_{ij}) \tag{1}$$

where $\phi(r_{ij})$ is the interaction potential and $r_{ij} = |\boldsymbol{r}_i - \boldsymbol{r}_j|$. As a consequence the Newton's equations result[9]

$$m_i\ddot{\boldsymbol{r}}_i = \sum_{i\neq j}\frac{1}{r_{ij}}\frac{\mathrm{d}\phi(r_{ij})}{\mathrm{d}r_{ij}}\boldsymbol{r}_{ij} \tag{2}$$

and must be solved numerically[9~12].

The statistical averages of interest must be calculated as temporal averages over the trajectories of the system in its phase space. The bulk system can be simulated by periodic boundary conditions[10]. These can be obtained by periodically repeating a unit cell of volume Ω, containing N particles, by translations[4,10]. The solution of Eq. (2) conserves the total energy E of the system, so the statistical ensamble generated in molecular dynamics is a microcanonical ensamble[4,12,13].

2 PARRINELLO-RAHMAN MODEL

Let us consider a system as defined in section 1. It is simulated by a cell repeated to fill all space. The cell can have arbitrary shape and volume, completed described by three vectors $\boldsymbol{a}$, $\boldsymbol{b}$ and $\boldsymbol{c}$ which span the edges of the molecular dynamics cell. Following Parrinello and Rahman[4], the 3×3 matrix $\boldsymbol{h}$ whose solumns are respectively the components of $\boldsymbol{a}$, $\boldsymbol{b}$ and $\boldsymbol{c}$ can be introduced to describe the solid structure[4]. As a consequence the volume of the cell results

$$\Omega = |\det\boldsymbol{h}| = \boldsymbol{a}\cdot\boldsymbol{b}\wedge\boldsymbol{c} \tag{3}$$

The position $\boldsymbol{r}_i$ of the i-th particle can be written in terms of $\boldsymbol{h}$ and of a column vector $\boldsymbol{s}_i \equiv (\xi_i, \eta_i, \zeta_i)$, with $0\leqslant\xi_i\leqslant1, 0\leqslant\eta_i\leqslant1, 0\leqslant\zeta_i\leqslant1$ and $i = 1, \cdots, N$, as follows

$$\boldsymbol{r}_i = \boldsymbol{h}\boldsymbol{s}_i = \xi_i\boldsymbol{a} + \eta_i\boldsymbol{b} + \zeta_i\boldsymbol{c} \tag{4}$$

In the analysis of the elastic body a reference state of the system must be defined. Following Parrinello and Rahman[4] it can be defined by a reference tensor $\boldsymbol{h}_0$ and a reference volume $\Omega_0 = |\det\boldsymbol{h}_0|$, and a reference position $\boldsymbol{r}_0$ defined as follows

$$\boldsymbol{r}_0 = \boldsymbol{h}_0\boldsymbol{s} \tag{5}$$

whose components are denoted by x_u[4].

A homogeneous distorsion of the system changes $\boldsymbol{h}_0$ to $\boldsymbol{h}$, moving $\boldsymbol{r}_0$ to $\boldsymbol{r} = \boldsymbol{h}\boldsymbol{s} = \boldsymbol{h}\boldsymbol{h}_0^{-1}\boldsymbol{r}_0$[4], causing the displacement $\boldsymbol{u}$ due to the distorsion itself[14]

$$\boldsymbol{u} = \boldsymbol{r} - \boldsymbol{r}_0 = (\boldsymbol{h}\boldsymbol{h}_0^{-1} - \boldsymbol{I})\boldsymbol{r}_0 \tag{6}$$

Now, introducing the metric tensor $\boldsymbol{G}$

$$\boldsymbol{G} = \boldsymbol{h}^+\boldsymbol{h} \tag{7}$$

where $\boldsymbol{h}^+$ is the transposed of $\boldsymbol{h}$, the strain tensor $\boldsymbol{E} = (\mathrm{grad}\boldsymbol{u}^+ + \mathrm{grad}\boldsymbol{u})/2$, whose components are[14]

$$\varepsilon_{\lambda\mu} = \frac{1}{2}\left(\frac{\partial u_\lambda}{\partial x_\mu} + \frac{\partial u_\mu}{\partial x_\lambda} + \sum_v\frac{\partial u_v}{\partial x_\mu} + \frac{\partial u_v}{\partial x_\lambda}\right) \tag{8}$$

can be defined as follows[4]

$$\boldsymbol{E} = \frac{1}{2}(\boldsymbol{h}_0^{+-1}\boldsymbol{G}\boldsymbol{h}_0^{-1} - \boldsymbol{I}) \tag{9}$$

Let $\boldsymbol{S}$ be the stress tensor, mathematically represented by the first Piola-kirchhoff tensor[3], and p the hydrostatic pressure[4], the elastic energy V_{el} results[4]

$$V_{el} = p(\Omega - \Omega_o) + \Omega_0 \mathrm{tr}[(\boldsymbol{S} - p\boldsymbol{I})\boldsymbol{E}] \tag{10}$$

where tr represents the trace of the tensor $\boldsymbol{X}$.

Now the elastic Lagrangian L can be introduced[4]

$$L = \frac{1}{2}\sum_{k=1}^{N} m_k \dot{\boldsymbol{s}}_k^{+}\boldsymbol{G}\dot{\boldsymbol{s}}_k - \sum_{k=1}^{N}\sum_{i>k}^{N}\phi(r_{ki}) + \frac{1}{2}W\mathrm{tr}[\dot{\boldsymbol{h}}^{+}\dot{\boldsymbol{h}}] - p\Omega_0 - \frac{1}{2}\mathrm{tr}[\boldsymbol{\Sigma}\boldsymbol{G}] \tag{11}$$

where W can be chosen on the basis of computational convenience[15] and the tensor $\boldsymbol{\Sigma}$ is defined as follows[4]

$$\boldsymbol{\Sigma} = \Omega_0 \boldsymbol{h}_0^{+-1}(\boldsymbol{S} - p\boldsymbol{I})\boldsymbol{h}_0^{-1} \tag{12}$$

From this expression of the elastic Lagrangian Parrinello and Rahman obtained the following dynamic equations[4]

$$\begin{cases} \ddot{\boldsymbol{s}}_k = -\sum_{i\neq k}\dfrac{\mathrm{d}\phi(r_{ki})}{\mathrm{d}r_{ki}}\dfrac{\boldsymbol{s}_k - \boldsymbol{s}_i}{r_{ki}} - \boldsymbol{G}^{-1}\dot{\boldsymbol{G}}\dot{\boldsymbol{s}}_k & \text{with } k = 1, \cdots, N \\ W\ddot{\boldsymbol{h}} = (\boldsymbol{\pi} - p\boldsymbol{I})\boldsymbol{\sigma} - \boldsymbol{h}\boldsymbol{\Sigma} \end{cases} \tag{13}$$

with

$$\boldsymbol{\sigma} = \Omega \boldsymbol{h}_0^{+-1} \tag{14}$$

and

$$\boldsymbol{\pi}_{\alpha\beta} = \Omega^{-1}\sum_{k=1}^{N} m_k[(\boldsymbol{h}\dot{\boldsymbol{s}}_k)^{+}(\boldsymbol{h}\dot{\boldsymbol{s}}_k)]_{\alpha\beta} + \Omega^{-1}\sum_{k=1}\sum_{i>k}\left(\frac{\mathrm{d}\phi(r_{ki})}{\mathrm{d}r_{ki}}\boldsymbol{h}\frac{\boldsymbol{s}_k - \boldsymbol{s}_i}{r_{ki}}\right)_{\alpha\beta} \tag{15}$$

3 THERMOELASTIC BODIES

In section 1 an introduction to molecular dynamics has been presented. In section 2 the results of Parrinello and Rahman have been summerised. Now a general thermodynamic analysis of the linear thermoelastic bodies will be developed.

Considering a continuum body[16] and assuming that the bound region of space occupied by the body is in a fixed reference configuration, closed with respect to mass transfer and open with respect to energy transfer, as described in section 2. This body is a thermodynamic closed system[3,5,6]. According to Carlson[3,17] the first law of thermodynamics can be written as

$$\rho c\frac{\mathrm{d}T}{\mathrm{d}t} = \mathrm{T}\frac{\partial \boldsymbol{S}}{\partial T}\frac{\mathrm{d}\boldsymbol{D}}{\mathrm{d}t} - \mathrm{div}\boldsymbol{q} + \rho\Xi \tag{16}$$

where ρ——Mass density

c——Specific heat

T——Temperature

$\boldsymbol{q}$——Heat flux

Ξ——Inner thermal source[5]

$\boldsymbol{D}$——Finite strain tensor defined in function of the strain tensor $\boldsymbol{E}$ and of the displacement $\boldsymbol{u}$ as follows[3,16,17]

$$\boldsymbol{D} = \boldsymbol{E} + \frac{1}{2}\mathrm{grad}\boldsymbol{u}^{+}\boldsymbol{u} \tag{17}$$

Assuming the isotropy of the body the constitutive equation results[3,17]

$$\boldsymbol{S} = 2u\boldsymbol{E} + [\lambda \mathrm{tr}\boldsymbol{E} - \beta(T - T_0)]\boldsymbol{I} \tag{18}$$

where u and λ are the Lame moduli and $\beta = (3\lambda + 2\mu)\alpha$, with α linear thermal expansion coefficient[16,17]. From experimental data it has been noticed that the Lame moduli are functions of the temperature T[18,19].

From the relation Eq. (17) and the assumption of linear approximation for the gradient displacement it follows that[3]

$$\frac{\mathrm{d}\boldsymbol{D}}{\mathrm{d}t} \equiv \frac{\mathrm{d}\boldsymbol{E}}{\mathrm{d}t} \tag{19}$$

Now substituting the relation Eq. (18) in Eq. (16), using the relation Eq. (19), Eq. (16) itself results

$$\rho cb\frac{\mathrm{d}T}{\mathrm{d}t} = T\{2(\partial\mu/\partial T)\boldsymbol{E} + [(\partial\lambda/\partial T)\mathrm{tr}\boldsymbol{E} -$$

$$(\partial\beta/\partial T)(T - T_0) - \beta]\boldsymbol{I}\}\frac{\mathrm{d}\boldsymbol{E}}{\mathrm{d}t} = \mathrm{div}\boldsymbol{q} + \rho\Xi \tag{20}$$

From experimental results and from the analysis of the order of magnitude it has been pointed out that $[(\partial\beta/\partial T)(T - T_0)]$ is negligible with respect to β, $(\partial\mu/\partial T)\ \boldsymbol{E}$ and $(\partial\lambda/\partial T)$ tr $\boldsymbol{E}$. As a consequence, also assuming that the thermodynamic process is adiabatic, $\mathrm{div}\boldsymbol{q} = 0$, and that there are no internal sources, $\Xi = 0$[3,16~19], Eq. (20) results[3]

$$\frac{\rho c}{T}\frac{\mathrm{d}T}{\mathrm{d}t} = 2(\partial\mu/\partial T)\boldsymbol{E}\frac{\mathrm{d}\boldsymbol{E}}{\mathrm{d}t} + \{(\partial\lambda/\partial T)\mathrm{tr}\boldsymbol{E} - \beta\}\mathrm{tr}[\mathrm{d}\boldsymbol{E}/\mathrm{d}t] \tag{21}$$

which represents the thermoelastic relation between strain and temperature.

4 MODEL PROPOSED

In section 2 the molecular dynamic Eq. (13) of the elastic body have been obtained and in section 3 the thermophysical Eq. (21) have been determined. In this section the thermal behaviour of the body will be introduced in the Parrinello-Rahman model to obtain a termal molecular dynamic model useful in thermoelastic analysis of solids.

To that the differential Eq. (21) must be integrate, obtaining the following relation, expressed in components

$$T = T_0\exp\Big[\sum_{k=1}^{N}\sum_{i=1}^{N}\Big(\frac{1}{\rho c}\frac{\partial\mu}{\partial T} + \frac{1}{2\rho c}\frac{\partial\lambda}{\partial T}\delta_{ki}\Big)\varepsilon_{ki}^2 - \frac{\beta}{\rho c}\sum_{k=1}^{N}\varepsilon_{kk}\Big] \tag{22}$$

where T_0 is the temperature at the reference configuration, and from the relation Eq. (9)

$$\varepsilon_{\alpha\beta} = \frac{1}{2}(\boldsymbol{h}_0^{+-1}\boldsymbol{G}\boldsymbol{h}_0^{-1})_{\alpha\beta} - \frac{1}{2}\delta_{\alpha\beta} \tag{23}$$

Now, considering the relation Eq. (18), the expression Eq. (12) becomes

$$\sum = \Omega_0\boldsymbol{h}_0^{+-1}\{2\mu\boldsymbol{E} + [\lambda\mathrm{tr}\boldsymbol{E} - \beta(T - T_0) - p]\boldsymbol{I}\}\boldsymbol{h}_0^{-1} \tag{24}$$

where $T - T_0$ is expressed by the relation Eq. (22) as follows

$$T - T_0 = T_0\exp\Big[\sum_{k=1}^{N}\sum_{i=1}^{N}\Big(\frac{1}{\rho c}\frac{\partial\mu}{\partial T} + \frac{1}{2\rho c}\frac{\partial\lambda}{\partial T}\delta_{ki}\Big)\varepsilon_{ki}^2 - \frac{\beta}{\rho c}\sum_{k=1}^{N}\varepsilon_{kk}\Big] - T_0 \tag{25}$$

In this way the thermal behaviour has been introduced in the Parrinello-Rahman model , obtaining the thermal molecular dynamic model useful in the analysis of the thermoelastic behaviour of solids. The

result obtained is that the evolution of the strain tensor can be obtained by the differential Eq. (13) coupled with the following equations

$$W[\ddot{\boldsymbol{h}}]_{\alpha\beta} = \sum_{k,\gamma} m_k [(\boldsymbol{h}\dot{\boldsymbol{s}}_k)^+ (\boldsymbol{h}\dot{\boldsymbol{s}}_k)]_{\alpha\gamma} [\boldsymbol{h}_0^{+-1}]_{\gamma\beta} - p\Omega [\boldsymbol{h}_0^{+-1}]_{\alpha\beta} +$$

$$\sum_{k,i>k,\gamma} \left(\frac{\mathrm{d}\phi(r_{ki})}{\mathrm{d}r_{ki}} \boldsymbol{h} \frac{\boldsymbol{s}_k - \boldsymbol{s}_i}{r_{ki}} \right)_{\alpha\gamma} [\boldsymbol{h}_0^{+-1}]_{\gamma\beta} - \mu\Omega_0 \sum_{\gamma} [\boldsymbol{h}]_{\alpha\gamma} [\boldsymbol{h}_0^{+-2} \boldsymbol{G} \boldsymbol{h}_0^{-2}]_{\gamma\beta} +$$

$$\beta T_0 \Omega_0 \exp\Big[\sum_{k=1}^{N} \sum_{i=1}^{N} \left(\frac{1}{\rho c} \frac{\partial \mu}{\partial T} + \frac{1}{2\rho c} \frac{\partial \lambda}{\partial T} \delta_{ki} \right) \varepsilon_{ki}^2 - \frac{\beta}{\rho c} \sum_{k=1}^{N} \varepsilon_{kk} \Big] \sum_{\gamma} [\boldsymbol{h}]_{\alpha\gamma} [\boldsymbol{h}_0^{+-1} \boldsymbol{h}_0^{-1}]_{\gamma\beta} -$$

$$\left[\beta T_0 + \lambda \left(\sum_k \varepsilon_{kk} \right) - p - \mu \right] \Omega_0 \sum_{\gamma} [\boldsymbol{h}]_{\alpha\gamma} [\boldsymbol{h}_0^{+-1} \boldsymbol{h}_0^{-1}]_{\gamma\beta} \tag{26}$$

where $\varepsilon_{\alpha\beta}$ and $\boldsymbol{G}$ are respectively expressed by Eq. (23) and Eq. (7).

5 CONCLUSIONS

The thermal behaviour of a solids under elastic deformations has been analysed obtaining a model which combines the molecular dynamics results with the global thermal behaviour of the solid itself in order to develop a numerical method of analysis of the thermoelasticity.

To do that in section 1 an introduction to molecular dynamics has been presented, in section 2 the results of Parrinello and Rahman has been summerised, in section 3 the thermodynamic analysis of the linear thermoelastic bodies has been developed and, finally, in section 4 the thermoelastic molecular dynamic model has been obtained.

The result obtained consists of the introduction of the thermal behaviour in the Parrinello-Rahman model, obtaining the thermal molecular dynamic model useful in the analysis of the thermoelastic behaviour of solids. This model is mathematically expressed by Eq. (13) coupled with Eq. (26) numerically calculable.

References

1 Heath K D, Mackrodt W C, Saunders V R, et al. Calculated enthalpies of mixing of MnO/MgO and NiO/MgO. J. Mater. Chem, 1994, 4(6): 825 ~ 829

2 Lucia U, Causa M. The maximum entropy variation and the calculation of the lattice constant. Il Nuovo Cimento, 1998, D 20: 807 ~ 810

3 Bonadies M, Lucia U, Pastrone F. Thermoelastic stress analysis for linear thermoelastic bodies. Books of the Ma – thematical Department of the University of Torino. Book n. 1/1998

4 Parrinello M, Rahman A. Polymorphic transitions in single crystals: a new molecular dynamics method. J. Appl. Phys., 1981, 52(12): 58 ~ 66

5 Lucia U. Mathematical consequences of the Gyarmati's principle in rational thermodynamics. Il Nuovo Cimento B 110, 1995, 10: 1 227 ~ 1 235

6 Lucia U, Grazzini G. Global analysis of dissipation due to irreversibility. Rev. Gén. Therm., 1997, 36: 605 ~ 609

7 Lucia U. Maximum entropy and open systems including two phase flows. Rev. Gén. Therm., 1998, 37: 813 ~ 817

8 Schiff L I. Quantum Mechaoics. New York: McGraw-Hill, 1968

(Continued on page 177)

OPTIMAL FEED RATE CONTROL FOR MULTI-AXIS CNC MACHINING OF FREE FORM SURFACES①

Zhan Yong Zhou Ji Zhou Yanhong Zhou Yunfei
School of Mechanical Science and Engineering,
Huazhong University of Science and Technology

Abstract Considering machining efficiency, surface quality and wear of cutter and machine, it is necessary to maintain high, stable and constant surface feed rate as far as possible. The feed rate control strategy for multi-axis CNC machining of free-form surfaces is presented. It comprises: ①the determination of effective feed rate; ② the adoption of suitable approaches to smooth feed rate. This strategy considers path geometry, actuator limitation and machine dynamics. The result shows that machining efficiency is improved effectively.

Key words: CNC Surface machining Feed rate Multi-axis

0 INTRODUCTION

The magnitude of feed rate determines machining efficiency. Generally constant feed rate machining generates relatively better surface quality than non-constant feed rate cases. In addition, the acute variation of feed rate leads to severe wear of cutter and machine. Therefore, considering these aspects, it is necessary to maintain high, stable and constant surface feed rate (namely the feed rate of cutter on the machining position against workpiece surface) as far as possible. On the other hand, the surface geometry is complicated, constant surface feed rate suffers continuous variations of velocities of moving axes. These variations cause excessive velocities and accelerations resulting in tracking error. Furthermore it is desirable to adjust code feed rate in terms of the actuator limitation and machine dynamics.

However, there are some weaknesses in current feed rate control for surface machining in which surfaces are often generated as a sequence of discrete minor segments: ① In the programming, it is customary to determine feed rate according to the constant motion of cutter on the offset surface, so surface feed rate is not constant. Furthermore, it is seldom to consider the designed path geometry, the assigned actuator limitation and the given machine dynamics. ② In CNC control, CNC only executes the code feed rate of each program segment faithfully, frequent deceleration and acceleration suffered from minor segments make it very difficult to maintain the code feed rate constantly[1~4].

Supported financially by National Natural Science Foundation of China and the Eight-Five Year Plan National Key Projeets the task group with authors has developed a CNC system for surface direct interpolation. In this system, the feed rate can be determined and controlled by synthesizing the following factors: ①The surface feed rate is kept be constant as far as possible. ②The velocities and accelerations of each moving axis should not exceed the actuator limitation. ③The feed rate should change smoothly in the portions of transition and stop-start motion.

①This project is supported by National Natural Science Foundation of China and the Eight-Five Year Plan National Key Projects. Manuscript received on October 9, 1999; revised manuscript March 27, 2000

需要全本请访问 www.ertongbook.com

1 BASIC STRATEGY

The aim of feed rate control strategy considers better surface quality as well as higher machining efficiency. It comprises: ①the determination of effective feed rate; ②the adoption of suitable approaches to smooth feed rate. Fig. 1 shows the feed rate control strategy adopted in our CNC system for surface direct interpolation.

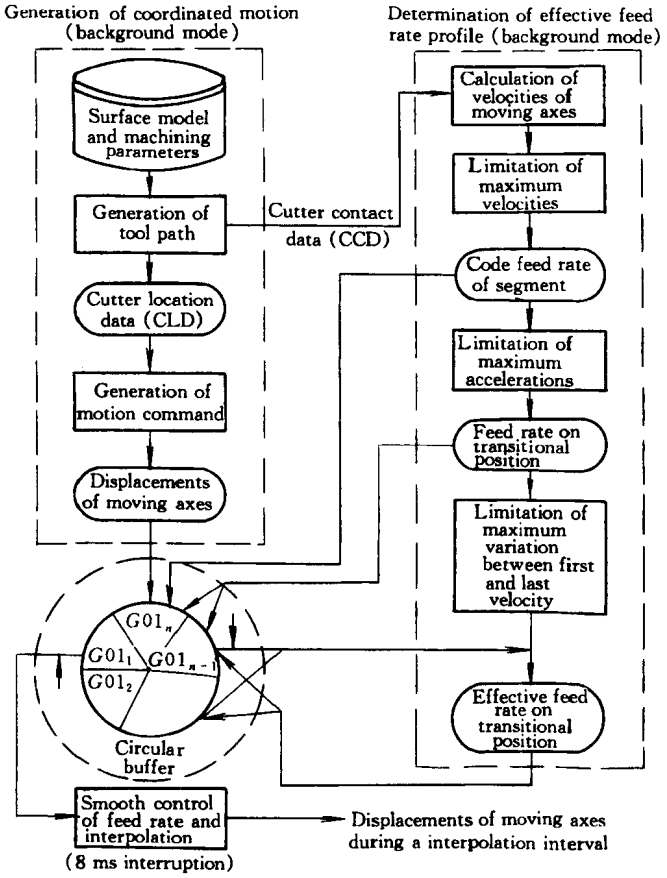


Fig. 1 Feed rate control strategy

2 GENERATION OF COORDINATED MOTION

Given a free form surface $\boldsymbol{r}_s(u, w)$, the path generated in various machining ways has the following common form: $\boldsymbol{r}_s(t) = \boldsymbol{r}_s(u(t), w(t))$. As shown in Fig. 2, for five-axis machining with general cutters such as ball end cutter, flat end cutter, torus cutter, drum cutter and so on, the cutter location (CL) path in workpiece coordinate system (WCS) can be expressed in a general form

$$\begin{cases} \boldsymbol{I}_a(t) = \sin\alpha \boldsymbol{I}_{ft}(t) + \cos\gamma \boldsymbol{I}_n(t) \pm (\sin^2\gamma - \sin^2\alpha)^{1/2} \boldsymbol{I}_v(t) \\ \boldsymbol{r}_p(t) = \boldsymbol{r}(t) + (R_1 + b)\boldsymbol{I}_n(t) + (R_2 - R_1)[\boldsymbol{I}_n(t) - \cos\gamma \boldsymbol{I}_a(t)]/|\boldsymbol{I}_n(t) - \cos\gamma \boldsymbol{I}_a(t)| \end{cases} \quad (1)$$

where $\boldsymbol{I}_a(t)$——Unit vector of cutter axis

$\boldsymbol{r}_p(t)$——Positional vector of CL point P

$\boldsymbol{I}_{ft}(t)$——Unit tangential vector in machining direction $\boldsymbol{I}_v(t) = \boldsymbol{I}_n(t) \times \boldsymbol{I}_{ft}(t)$

$\boldsymbol{I}_n$——Unit normal vector of surface

α——Lead angle γ——Tilt angle

R_2, R_1——Parameters of cutter b——Machining allowance

For the five-axis type of machine with Euler-angle rotary structure as shown in Rig. 2, given that axis A is installed on axis B and A intersect B perpendicularly, rotation of B and A are $\varphi(t)$ and $\theta(t)$ respectively. And translation of machine can be considered as motion of swinging center P_s, let it be $\boldsymbol{r}_{Ps}(t) = (x_{Ps}(t), y_{Ps}(t), z_{Ps}(t))$. Suppose $\varphi(t)$ and $\theta(t)$ are zero in inital state, A and B are aligned with x and z respectively, then

$$\begin{cases}\theta(t) = \arccos i_{az}(t) \\ \varphi(t) = \arctan[-i_{ax}(t)/i_{ay}(t)]\end{cases} \tag{2}$$

$$\boldsymbol{r}_{Ps}(t) = \boldsymbol{r}_o + \boldsymbol{r}_p(t) + l\boldsymbol{I}_a(t) \tag{3}$$

where $i_{ax}(t), i_{ay}(t), i_{az}(t)$——Coordinates of $\boldsymbol{I}_a(t)$ in WCS

$\boldsymbol{r}_o$——Positional vector of origin of WCS in machine coordinate system

l——Distance between CL point P and swinging center P_s

$l\boldsymbol{I}_a(t)$——Additional translational ve - ctor resulting from rotation or swing of machine

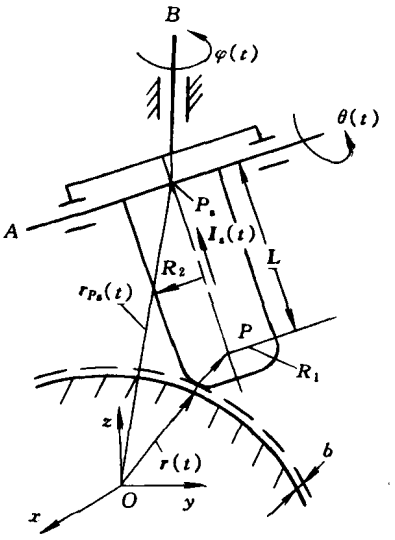


Fig.2 Five-axis machining with Euler-angle rotary structure

For the five-axis machine as shown in Fig. 2, the ideal successive coordinated motion can be given in Eqs. (2) and (3). Because CNC system only processes discrete data, the generation of coordinated motion means to seek a sequence of parametericvalues $(t_0, t_1, \cdots)$ which satisfy the assigned approximating accuracy of path, then $\boldsymbol{r}_s(t_k)$, $(\boldsymbol{I}_a(t_k), \boldsymbol{r}_p(t_k))$ and $(\Delta\boldsymbol{r}_{Ps}(t_k), \Delta\varphi(t_k), \Delta\theta(t_k))$ can be obtained from $\boldsymbol{r}_s(t)$ and Eqs. (1) ~ (3), where $k = 0, 1, \cdots$. Between two neighbouring discrete positions, the coordinated motion is linear, thus workpiece program is made up of linear program segments. Let $\Delta\boldsymbol{r}_{sk} = \boldsymbol{r}_s(t_{k+1}) - \boldsymbol{r}_s(t_k)$, $\Delta\boldsymbol{r}_{Psk} = \boldsymbol{r}_{Ps}(t_{k+1}) - \boldsymbol{r}_{Ps}(t_k)$, $\Delta\varphi_k = \varphi(t_{k+1}) - \varphi(t_k)$, $\Delta\theta_k = \theta(t_{k+1}) - \theta(t_k)$, where $k = 0, 1, \cdots$, $\Delta\boldsymbol{r}_{sk}$ and $(\Delta\boldsymbol{r}_{Psk}, \Delta\varphi_k, \Delta\theta_k)$ are increments of cutter contact(CC)piont and moving axes in the kth segment respectively.

3 GENERATION OF EFFECTIVE FEED RATE PROFILE

3.1 Velocities of moving axes result from constant surface feed rate

For program segment $G01_k$, the increments of moving axes(x, y, z, a, b) are $(\Delta x_{Psk}, \Delta y_{Psk}, \Delta z_{Psk}, \Delta\theta_k, \Delta\varphi_k)$, the increment of corresponding CC point is $\Delta\boldsymbol{r}_{sk}$, the code feed rate is u_k, then the velocities of moving axes$(v_{xk}, v_{yk}, v_{zk}, v_{ak}, v_{bk})$ can be expressed as

$$\begin{cases}v_{xk} = v_k \Delta x_{Psk}/|\Delta\boldsymbol{r}_{sk}| \\ v_{yk} = v_k \Delta y_{Psk}/|\Delta\boldsymbol{r}_{sk}| \\ v_{zk} = v_k \Delta z_{Psk}/|\Delta\boldsymbol{r}_{sk}| \\ v_{ak} = v_k \Delta\theta_k/|\Delta\boldsymbol{r}_{sk}| \\ v_{bk} = v_k \Delta\varphi_k/|\Delta\boldsymbol{r}_{sk}|\end{cases} \tag{4}$$

Obviously, the composed velocity determined by Eq. (4) can make cutter motion at feed rate v_k.

3.2 Limitation of feed arte

In the places of surface with big curvature, cutter axis vector $\boldsymbol{I}_a(t)$ will vary sharply. From Eq. (1) ~ Eq. (4), this will make the velocity and acceleration of rotary/swing axis increase. It is more serious that the additional translational vector $l\Delta\boldsymbol{I}_{ak}$, which results from the rotation/swing of machine and path geometry, will lead to excessive velocity and acceleration of translational axis for comparatively big swing radius l

(maching concave surface will lead to extremely slow translational velocity). Therefore, it is necessary to adjust the code feed rate automatically according to the machine dynamics and actuator ability.

3.2.1 Limitation of maximum velocity of moving axes

The velocities of moving axes obtained from Eq. (4) can not exceed the allowable maximum velocities, that is

$$|v_{\Lambda k}| \leqslant v_{\Lambda \max} \qquad \Lambda = x, y, z, a, b \tag{5}$$

If one velocity can not satisfy Eq. (5), the velocities of moving axes must be adujsted in terms of the designed tool path, in other words, the feed rate v_k must be asjusted. For example, if v_{xk} exceeds $v_{x\max}$, v_k has to be adjusted as

$$v_k = v_{x\max} |\Delta \boldsymbol{r}_{sk}| / |\Delta x_{Psk}| \tag{6}$$

3.2.2 Limitation of maximum acceleration on transitional position

From Eq. (4), if the direction and magnitude of feed rate between neighboring segments change, the direction and magnitude of moving axis may vary sharply. To achieve the assigned approximating accuracy of path and avoid the shock of machine tool, the acceleration of any moving axis on the transitional position (the intersection of neighboring segments) can not exceed the ability of servo driving. Let v_{kj}, $v_{\Lambda kb}$ and $v_{\Lambda(k-1)e}$ be the feed rate on the transitional position of the kth and $k-1$th segment, the velocity of each moving axis on the start position (during the first interpolation interval) of the kth segment and the velocity on the end position (during the last interpolation interval) of the $k-1$th segment respectively, then the accelerations of moving axes during neighboring interpolation interval should satisfy the following equation

$$|v_{\Lambda kb} - v_{\Lambda(k-1)e}| / T_s \leqslant a_{\Lambda \max} \qquad \Lambda = x, y, z, a, b \tag{7}$$

where $a_{\Lambda\max}$——Maximum acceleration or deceleration

T_s——Interpolation interval of CNC system

Firstly, let v_{kj} equal to v_k, if Eq. (7) can not be satisfied, v_{kj} should be limited based on Eq. (4) and Eq. (7). For example, the acceleration of axis x can not satisfy Eq. (7), v_{kj} should be adjusted as

$$v_{kj} = a_{x\max} T_s / \left| \frac{\Delta x_{Ps\,k+1}}{\Delta \boldsymbol{r}_{s\,k+1}} - \frac{\Delta x_{Psk}}{\Delta \boldsymbol{r}_{sk}} \right| \tag{8}$$

3.2.3 Limitation of maximum variation between the first and last velocity in deceleration segment

Let the circular buffer store previous n linear segments

$$G01_k(\Delta \boldsymbol{r}_{sk}, \Delta \boldsymbol{r}_{Psk}, \Delta\theta_k, \Delta\varphi_k, v_k, v_{kj}, v_{k+1\,j}) \qquad k = 1, 2, \cdots, n$$

For the segment $G01_k$, if v_{kj} is larger than $v_{(k+1)j}$, this segment is a deceleration segment. Because the segment length $|\Delta \boldsymbol{r}_{sk}|$ is limited, the variation between v_{kj} and $v_{k+1\,j}$ must be restricted within the range allowed by servo driving ability of machine. In other words, v_{kj} must be decreased because it is impossible to raise $v_{k+1\,j}$. Suppose the exponential law is followed during the course of deceleration, the deceleration distance from v_{kj} to $v_{k+1\,j}$ can be expressed as

$$d_k = \int_0^\infty v_{kj} \exp(-t/\tau)\,dt - \int_0^\infty v_{(k+1)j} \exp(-t/\tau)\,dt = (v_{kj} - v_{(k+1)j})\tau \tag{9}$$

where τ——Comprehensive time constant of technology system

Obviously, d_k should not exceed $|\Delta \boldsymbol{r}_{sk}|$, otherwise v_{kj} should be adjusted as

$$v_{kj} = |\Delta \boldsymbol{r}_{sk}| / \tau + v_{k+1\,j} \tag{10}$$

The feed rate of start position should be one by one verified and adjusted based on this limitation in inverse sequence (that is, $G01_n \rightarrow G01_{n-1} \rightarrow \cdots \rightarrow G01_2$) until one segment can not satisfy this condition. So the deceleration can be moved up to realize the stable motion of machine. From this process, the length

of circular buffer should satisfy that the code feed rate of the first segment (the current segment $G01_1$) can not be affected in the condition that the last segment $G01_n$ is regarded as the termination of path.

3.3 Smooth control of feed rate

From the above analysis, because of the path geometry, the machine dynamics, the servo driving ability and the effect of stop-start motion, the feed rate of machine may change. Thus it is necessary to adopt suitable measures for acceleration and deceleration to avoid the shock of machine which leads to tracking error and wear of cutter and machine.

Through the process of last section, the start position feed rate, the end position feed rate and the effective feed rate of each segment have been obtained. On this basis, the comparatively smooth exponential law is followed during the deceleration and acceleration in this system.

For the current segment $G01_1$ in buffer, the feed rate curve following the index law from v_{1j} accelerating to v_1 can be expressed

$$v(t) = v_1 - (v_1 - v_{1j})\exp(-t/\tau) \tag{11}$$

and the curve from the current feed rate v_q decelerating to v_{2j} can be expressed

$$v(t) = v_q \exp(-t/\tau) \tag{12}$$

CNC system processes the acceleration or deceleration in the way of discrete sampling at the moment $t = T_s, 2T_s, 3T_s, \cdots$. And $\exp(-(q+1)T_s/\tau) = C \cdot \exp(-qT_s/\tau)$, where $C = \exp(-T_s/\tau)$ is a constant, so the feed rate during the acceleration and deceleration can be obtained through iterative calculation without exponential calculation. During the qth interpolation interval, the condition of beginning deceleration is that v_q exceeds v_{2j} and the remaining length of this code segment L_q has been smaller than deceleration distance d_q between v_q and v_{2j}. From Eq. (9), we obtain $d_q = (v_q - v_{2j})\tau$. Then the algorithm of exponential acceleration or deceleration can be expressed as follows

if	$(v_q > v_{2j} \&\& L_q < (v_q - v_{2j})\tau)$	$v_{q+1} = v_q C$
else if	$(v_q < v_1)$	$v_{q+1} = v_1 + (v_q - v_1)C$
else		$v_{q+1} = v_1$
if	$(v_{q+1} < v_m)$	$v_{q+1} = v_m$

where v_m is allowable sudden feed rate of stop-start motion. Thus the velocities of moving axes can be obtained from Eq. (4), furthermore the increments of moving axes during an interpolation interval can be calculated and output.

4 EXPERIMENTS AND CONCLUSIONS

The above feed rate control strategy based on surface direct interpolation has been realized in PC-based CNC system developed in-house. We obtain the good effect in the machining of practical workpieces such as wave wheel of washing machine, blade of air-blower and integral centrifugal impeller etc. Machining efficiency can be illustrated by the following experimental results. A CC path and relevant CL path of the surface to be machined are depicted in Fig. 3. Specifications of Euler-angle rotary structure five-axis machine tool are: $R_2 = 5$ mm, $R_1 = 0$, $l = 200$ mm, the maximum velocity of translation axis 100 mm/s, the maximum acceleration of translation axis 120 mm/s^2, the maximum velocity of rotary axis 3 r/s, the maximum acceleration of rotary axis 4 r/s^2, the time constant 0.2 s, the interpolation interval 0.008 s.

For the assigned approximating accuracy 0.005 mm and the code feed rate 25 mm/s, Fig.4 shows the feed rate profile processed with the common method in which acceleration and deceleration are method introduced in this paper is shown in Fig. 5. Feed rate has t processed in each linear segment, the total machining time is 231.30 s. While the profile processed with the o be adjusted in some places where curvatures vary sharply, and the machining time is only 34.55 s. The velocities and accelerations of x, y, z axes are plotted in Fig. 6 and Fig. 8 respectively. Fig. 7 and Fig. 9 show the velocities and accelerations of a, b axes.

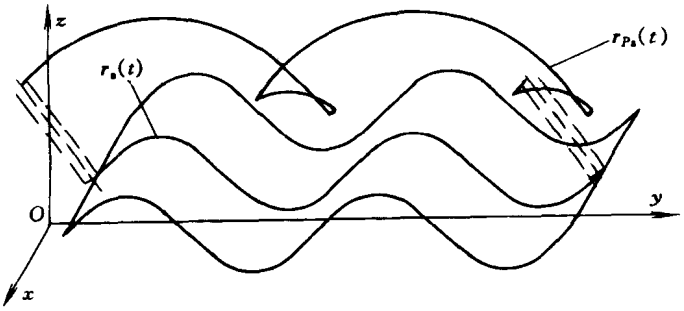


Fig.3 CC path and relevant CL path

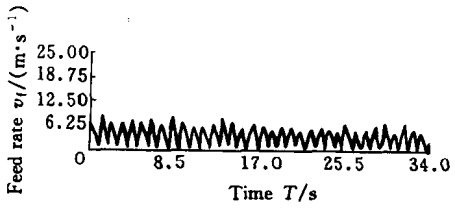


Fig.4 Feed rate profile 1

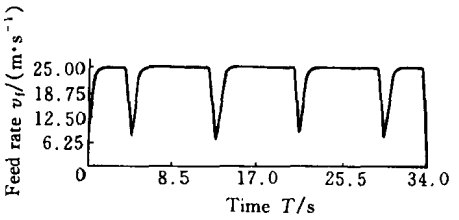


Fig.5 Feed rate profile 2

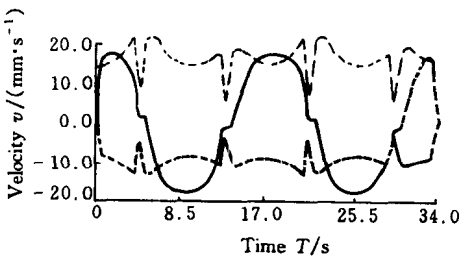


Fig.6 Velocities of x, y, z
Solid line——x axis Dotted line——y axis
Dashed line——z axis

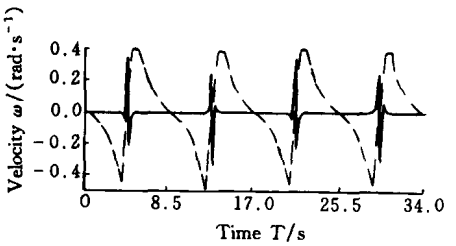


Fig.7 Velocities of a, b
Dotted line——a axis
Solid line——b axis

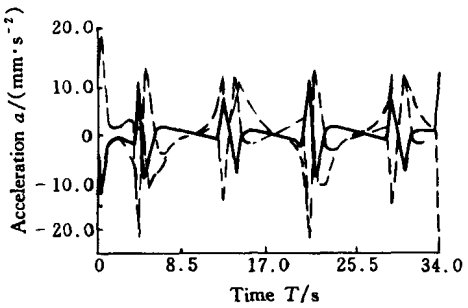


Fig.8 Accelerations of x, y, z
Solid line——x axis Dotted line——y axis
Dashed line——z axis

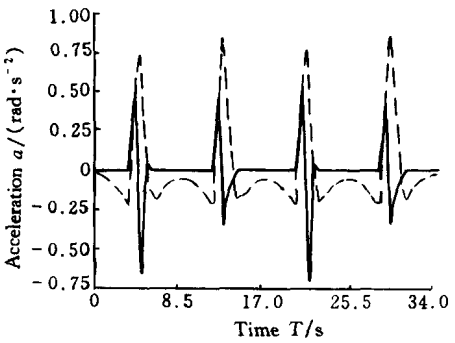


Fig.9 Accelerations of a, b
Dotted line——a axis
Solid line——b axis

It is thus clear: the method introduced in this paper can realize the optimal control of feed rate according to path geometry, machining dynamics and actuator limitation. We believe that it is very significant to raise machining efficiency, surface quality and life of cutter and machine.

References

1 Shpitalni M, Koren Y, Lo C C. Real-time curve interpolator. Computer-Aided Design, 1994, 26(11): 832 ~ 838

2 Daniel C H Yang, Tom Kong. Parametric interpolator versus linear interpolator for precision CNC machining. Computer-Aided Design, 1994, 26(3): 225 ~ 234

3 Dimitris Kiritsis. High precision interpolation algorithm for 3D parametric curve generation. Computer-Aided Design, 1994, 26(11): 850 ~ 855

4 Vickers G W, Bradley C. Curved surface machining through circular arc interpolation. Computers in Industry, 1992, 19: 329 ~ 337

(Continued from page 170)

9 Slater J C. Quantum Theory of Matter. New York: McGraw-Hill, 1968

10 Ashcroft N W, Mermin N D. Solid State Physics. New York: Harcourt Brace College Publisher (Saunders College Publishing), 1976

11 Hirsh D M. A Computational Approach to Chemistry. Blackwell Scientific Publication, 1994

12 Allen M P, Tildesley D J. Computer Simulation of Liquids. Oxford: Claredon Press, 1991

13 Hiu F L. An Introduction to Statistical Thermodynamics. Addison Wesley, 1960

14 Landau L D, Lifshitz E M. Theory of Elasticity. Oxford: Pergamon Press, 1959

15 Andersen H C, Chem J. Phys, 1980, 72: 2 384

16 Gurtin M E. The linear Theory of Elasticity, in Handbuck der Physik, Vla/2 Mechanics of Solids. Berlin: Springer, 1972

17 Carlson D E. Linear Thermoelasticity, in Handbuck der Physik, Vla/2 Mechanics of Solids. Berlin: Springer, 1972

18 Love A E H. A treatise on the Mathematical Theory of Elasticity. New York: Dover, 1927

19 Wong A K, Johnes R, Sparrow J G. Thermoelastic constant or thermoelastic parameter? J. Phys. Chem. Solids, 1987, 48, 8: 749 ~ 753

需要全本请访问 www.ertongbook.com